

Technische Universität Berlin
Institut für Mathematik

Model Order Reduction of
Nonlinear Circuit Equations

Andreas Steinbrecher and Tatjana Stykel

Preprint 2011/02

Preprint-Reihe des Instituts für Mathematik
Technische Universität Berlin

In this paper, we present a model order reduction approach for nonlinear circuit equations with a small number of nonlinear elements. This approach is based on the decoupling of linear and nonlinear subcircuits and reducing the linear part using balancing-related model reduction techniques. The efficiency and applicability of the proposed model reduction approach is demonstrated on numerical examples.

AMS(MOS) subject classification: 15A24, 34A09, 93C05, 94C99

Keywords: differential-algebraic equations, electronic circuits, modified nodal analysis, model reduction, balanced truncation, index

Model Order Reduction of Nonlinear Circuit Equations

Andreas Steinbrecher and Tatjana Stykel

May 3, 2011

Abstract

In this paper, we present a model order reduction approach for nonlinear circuit equations with a small number of nonlinear elements. This approach is based on the decoupling of linear and nonlinear subcircuits and reducing the linear part using balancing-related model reduction techniques. The efficiency and applicability of the proposed model reduction approach is demonstrated on numerical examples.

Keywords: differential-algebraic equations, electronic circuits, modified nodal analysis, model reduction, balanced truncation, index

AMS(MOS) subject classification: 15A24, 34A09, 93C05, 94C99

1 Introduction

The efficient and robust numerical simulation of integrated circuits plays a major role in computer-aided chip design. While the structural size of electronic devices is decreasing, their complexity is ever increasing. The mathematical modeling of such circuits leads to nonlinear systems of differential-algebraic equations (DAEs) containing up to millions or even more unknowns. Simulation of such large systems is mostly impossible or, at least, unacceptably time and storage consuming. Model order reduction provides a way out of this problem. A general idea of model reduction is to replace a large-scale system by a much smaller model which approximates the input-output relation of the original system within a required accuracy.

While a large variety of model reduction techniques such as PRIMA [13], SPRIM [6, 7] and PABTEC [17] exists for linear networks, model reduction of nonlinear circuits is only in its

*Institut für Mathematik, TU Berlin, Straße des 17. Juni 136, D-10623 Berlin, Germany; {steinbrecher, stykel}@math.tu-berlin.de. This work was supported by the Research Network SyreNe - *System Reduction for Nanoscale IC Design* funded by the German Federal Ministry of Education and Science (BMBF), grant no. 03STPAE3. Responsibility for the contents of this publication rests with the authors.

infancy [14, 19, 20, 23]. Typically, integrated circuits contain huge linear subnetworks modeling interconnects. A standard approach for model reduction of such nonlinear systems is to extract linear subsystems and replace them by reduced-order models, e.g., [5, 9, 13]. Then combining these reduced-order linear models with unchanged nonlinear components, one obtains a reduced-order nonlinear model that approximates the original system. The concept of this model reduction approach is presented in Figure 1. Although this approach is widely used in practice, only a little attention has been paid to approximation quality and properties of reduced-order nonlinear models.

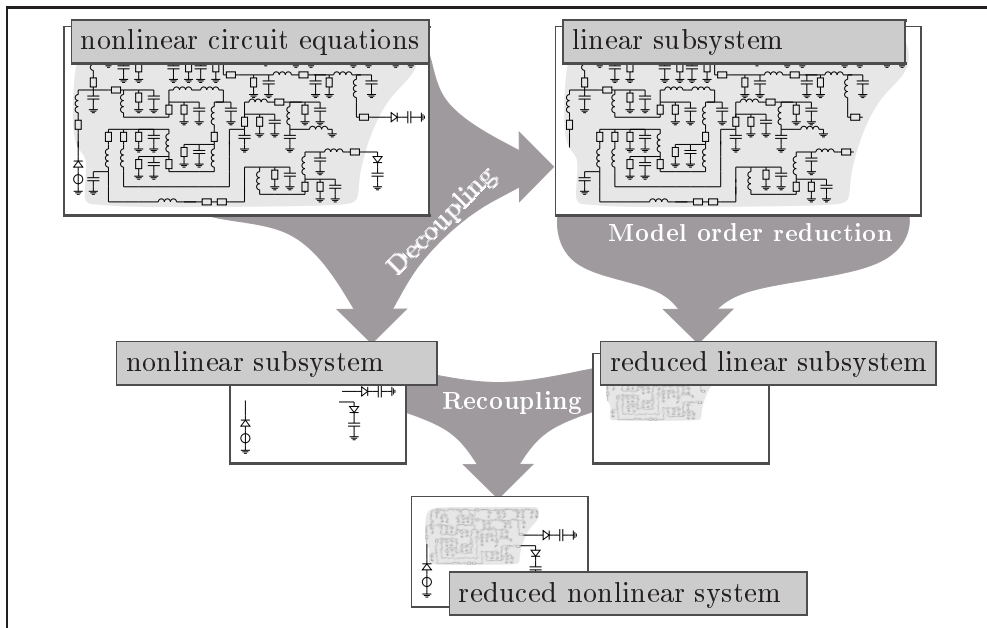


Figure 1: Model order reduction strategy for nonlinear circuits

In [9], model reduction based on partitioning linear and nonlinear subnetworks for a special class of RLC circuits with only nonlinear resistors has been considered and global error bounds have been presented. In this paper, we consider model reduction of more general circuits that may contain other nonlinear elements like nonlinear capacitors, inductors and transistors. We restrict ourselves to circuits with a small number of nonlinear components. In this case, the extracted linear subcircuits have a small number of terminals, and they can be reduced by any known linear model reduction method. The separation of linear subnetworks from circuits containing many nonlinear elements will result in linear models with many inputs. For such systems, model order reduction can be combined with terminal reduction, e.g., [1, 4, 12].

The extraction of linear subsystems from a DAE system may lead to many unexpected effects such as index jump in the decoupled DAE subsystems or loss of regularity of the linear subsystem. This may then result in numerical instabilities, poor approximation and even failure of model reduction and simulation tools. In this paper, we develop a topology-based decoupling technique that avoids the increasing of the index and guarantees the

well-posedness of decoupled linear subsystems.

Another important issue in model reduction of electronic circuits via partitioning is the preservation of passivity and reciprocity in the reduced-order submodels. An interconnection of passive models is again passive meaning that the interconnected system does not generate energy [22]. Furthermore, passive and reciprocal systems can be realized as electrical circuits in a netlist format [10, 15, 25] that allows their transient analysis with standard circuit simulators. Therefore, for model reduction of linear subnetworks, we will use the passivity-preserving balanced truncation methods developed especially for electrical circuits in [17, 18]. An advantage of these methods over Krylov-type model reduction techniques is that they provide computable error bounds which can be used to estimate the approximation error for the reduced-order nonlinear system.

The paper is organized as follows. In Section 2, we briefly discuss the modeling of electrical circuits using the modified nodal analysis and present the circuit equations to be considered. In Section 3, we present a model reduction technique for nonlinear circuits based on partitioning linear and nonlinear subcircuits followed by reduction of the linear part. We also propose a decoupling strategy exploiting the topological structure of the circuit and investigate the properties of the decoupled systems. In Section 4, the efficiency of the proposed model reduction approach is demonstrated on numerical examples.

2 Circuit equations

A commonly used modeling tool for electrical circuits is the Modified Nodal Analysis (MNA) [24]. A circuit can be modeled as a directed graph whose edges correspond to the circuit elements like capacitors, resistors, inductors and transistors and whose nodes correspond to the interconnections of these elements. The topological structure of such a graph with $n_\eta + 1$ nodes and n_e edges can be described by an incidence matrix $\mathbf{A}_0 \in \{-1, 0, 1\}^{n_\eta+1, n_e}$ which has entries $a_{ij} = 0, -1$ and 1 depending on whether edge j is incident with node i and whether this edge leaves or enters node i . Using Kirchhoff's current and voltage laws as well as the branch constitutive relations, the dynamics of the circuit can be described by a DAE system of the form

$$\mathcal{E}(x) \frac{d}{dt} x = \mathcal{A} x + f(x) + \mathcal{B} u, \quad (1a)$$

$$y = \mathcal{B}^T x, \quad (1b)$$

where $x^T = [\eta^T \ i_\mathcal{L}^T \ i_\mathcal{V}^T]$, $u^T = [i_\mathcal{J}^T \ u_\mathcal{V}^T]$ and $y^T = [-u_\mathcal{J}^T \ -i_\mathcal{V}^T]$ are the state vector, input and output, respectively, and

$$\mathcal{E}(x) = \begin{bmatrix} A_C C (A_C^T \eta) A_C^T & 0 & 0 \\ 0 & \mathcal{L}(i_\mathcal{L}) & 0 \\ 0 & 0 & 0 \end{bmatrix}, \quad \mathcal{A} = \begin{bmatrix} 0 & -A_\mathcal{L} & -A_\mathcal{V} \\ A_\mathcal{L}^T & 0 & 0 \\ A_\mathcal{V}^T & 0 & 0 \end{bmatrix}, \quad (1c)$$

$$f(x) = \begin{bmatrix} -A_\mathcal{R} g(A_\mathcal{R}^T \eta) \\ 0 \\ 0 \end{bmatrix}, \quad \mathcal{B} = \begin{bmatrix} -A_\mathcal{J} & 0 \\ 0 & 0 \\ 0 & -I \end{bmatrix}. \quad (1d)$$

In these model equations, η is the vector of node potentials, $\iota_{\mathcal{L}}$, $\iota_{\mathcal{V}}$ and $\iota_{\mathcal{J}}$ are the vectors of currents through inductors, voltage sources and current sources, respectively, $u_{\mathcal{V}}$ and $u_{\mathcal{J}}$ are the vectors of voltages of voltage sources and current sources, respectively. The matrices $A_{\mathcal{C}} \in \mathbb{R}^{n_{\eta}, n_{\mathcal{C}}}$, $A_{\mathcal{L}} \in \mathbb{R}^{n_{\eta}, n_{\mathcal{L}}}$, $A_{\mathcal{R}} \in \mathbb{R}^{n_{\eta}, n_{\mathcal{R}}}$, $A_{\mathcal{V}} \in \mathbb{R}^{n_{\eta}, n_{\mathcal{V}}}$ and $A_{\mathcal{J}} \in \mathbb{R}^{n_{\eta}, n_{\mathcal{J}}}$ are the incidence matrices describing the topology of the corresponding circuit elements, where the subscripts \mathcal{C} , \mathcal{L} , \mathcal{R} , \mathcal{V} and \mathcal{J} stand for capacitors, inductors, resistors, voltage and current sources, respectively. Note that $\mathbf{A} = [A_{\mathcal{C}} \ A_{\mathcal{L}} \ A_{\mathcal{R}} \ A_{\mathcal{V}} \ A_{\mathcal{J}}]$ is a reduced incidence matrix obtained from \mathbf{A}_0 by removing a row corresponding to a ground node. Furthermore, the capacitance matrix-valued function $\mathcal{C} : \mathbb{R}^{n_{\mathcal{C}}} \rightarrow \mathbb{R}^{n_{\mathcal{C}}, n_{\mathcal{C}}}$, the inductance matrix-valued function $\mathcal{L} : \mathbb{R}^{n_{\mathcal{L}}} \rightarrow \mathbb{R}^{n_{\mathcal{L}}, n_{\mathcal{L}}}$ and the resistor relation $g : \mathbb{R}^{n_{\mathcal{R}}} \rightarrow \mathbb{R}^{n_{\mathcal{R}}}$ characterize the physical properties of the capacitors, inductors and resistors, respectively. The state vector has the dimension $n = n_{\eta} + n_{\mathcal{L}} + n_{\mathcal{V}}$, while the input and output vectors have the dimension $m = n_{\mathcal{J}} + n_{\mathcal{V}}$.

We will assume that the DAE system (1) is well-posed in the sense that

- (A1) the matrix $A_{\mathcal{V}}$ has full column rank,
- (A2) the matrix $[A_{\mathcal{C}} \ A_{\mathcal{L}} \ A_{\mathcal{R}} \ A_{\mathcal{V}}]$ has full row rank,
- (A3) the matrices $\mathcal{C}(A_{\mathcal{C}}^T \eta)$ and $\mathcal{L}(\iota_{\mathcal{L}})$ are symmetric, positive definite for all admissible η and $\iota_{\mathcal{L}}$,
- (A4) the function $g(A_{\mathcal{R}}^T \eta)$ is monotonically increasing for all admissible η .

Assumptions (A1) and (A2) imply that the circuit does not contain loops of voltage sources and cutsets of current sources, respectively, while assumptions (A3) and (A4) mean that all circuit elements are passive, i.e., they do not generate energy.

In the following, we will distinguish between linear circuit elements like linear resistors, capacitors and inductors, and nonlinear circuit elements like nonlinear capacitors, inductors, diodes and transistors. A circuit element is called linear if the current-voltage relation for this element is linear. Otherwise, the circuit element is called nonlinear. Without loss of generality we assume that the circuit elements are ordered such that the incidence matrices can be partitioned as

$$A_{\mathcal{C}} = [A_{\bar{\mathcal{C}}} \ A_{\tilde{\mathcal{C}}}], \quad A_{\mathcal{L}} = [A_{\bar{\mathcal{L}}} \ A_{\tilde{\mathcal{L}}}], \quad A_{\mathcal{R}} = [A_{\bar{\mathcal{R}}} \ A_{\tilde{\mathcal{R}}}], \quad (1e)$$

where the incidence matrices $A_{\bar{\mathcal{C}}}$, $A_{\bar{\mathcal{L}}}$ and $A_{\bar{\mathcal{R}}}$ correspond to the linear circuit components, and $A_{\tilde{\mathcal{C}}}$, $A_{\tilde{\mathcal{L}}}$ and $A_{\tilde{\mathcal{R}}}$ are the incidence matrices for the nonlinear devices. We also assume that the linear and nonlinear elements are not mutually connected, i.e.,

$$\mathcal{C}(A_{\mathcal{C}}^T \eta) = \begin{bmatrix} \bar{\mathcal{C}} & 0 \\ 0 & \tilde{\mathcal{C}}(A_{\tilde{\mathcal{C}}}^T \eta) \end{bmatrix}, \quad \mathcal{L}(\iota_{\mathcal{L}}) = \begin{bmatrix} \bar{\mathcal{L}} & 0 \\ 0 & \tilde{\mathcal{L}}(\iota_{\tilde{\mathcal{L}}}) \end{bmatrix}, \quad g(A_{\mathcal{R}}^T \eta) = \begin{bmatrix} \bar{g}(A_{\bar{\mathcal{R}}}^T \eta) \\ \tilde{g}(A_{\tilde{\mathcal{R}}}^T \eta) \end{bmatrix}, \quad (1f)$$

where $\bar{\mathcal{C}} \in \mathbb{R}^{n_{\bar{\mathcal{C}}}, n_{\bar{\mathcal{C}}}}$, $\bar{\mathcal{L}} \in \mathbb{R}^{n_{\bar{\mathcal{L}}}, n_{\bar{\mathcal{L}}}}$ and $\bar{g} \in \mathbb{R}^{n_{\bar{\mathcal{R}}}, n_{\bar{\mathcal{R}}}}$ are the capacitance, inductance and resistance matrices for the corresponding linear elements, whereas $\tilde{\mathcal{C}} : \mathbb{R}^{n_{\tilde{\mathcal{C}}}} \rightarrow \mathbb{R}^{n_{\tilde{\mathcal{C}}}, n_{\tilde{\mathcal{C}}}}$,

$\tilde{\mathcal{L}} : \mathbb{R}^{n_{\tilde{\mathcal{L}}}} \rightarrow \mathbb{R}^{n_{\tilde{\mathcal{L}}}, n_{\tilde{\mathcal{L}}}}$ and $\tilde{g} : \mathbb{R}^{n_{\tilde{\mathcal{G}}}} \rightarrow \mathbb{R}^{n_{\tilde{\mathcal{G}}}}$ describe the corresponding nonlinear components, and $v_{\tilde{\mathcal{L}}}$ is the vector of currents through the nonlinear inductors. It follows from assumptions (A3) and (A4) that the matrices \bar{C} , $\bar{\mathcal{L}}$ and \bar{G} are symmetric and positive definite, $\tilde{C}(A_{\tilde{C}}^T \eta)$ and $\tilde{\mathcal{L}}(v_{\tilde{\mathcal{L}}})$ are symmetric and positive definite for all admissible η and $v_{\tilde{\mathcal{L}}}$, and $\tilde{g}(A_{\tilde{\mathcal{R}}}^T \eta)$ is monotonically increasing for all admissible η .

The index concept plays an important role in the analysis of DAEs. To characterize different analytical and numerical properties of DAE systems, several index notations have been introduced in the literature, e.g., [2, 8, 11]. For example, the *differentiation index* is roughly defined as the minimum of times that all or part of a DAE system must be differentiated with respect to t in order to determine the derivative of x as a continuous function of t and x . In the following we will use the shorter term “index” instead of “differentiation index”.

It has been shown in [3] that the MNA system (1) satisfying assumptions (A1)-(A4) has index at most two. The index is zero if and only if $n_{\mathcal{V}} = 0$ and $\text{rank}(A_C) = n_{\eta}$. The following lemma gives equivalent conditions for the circuit to be of index one.

Lemma 2.1 *Consider a MNA system (1) that satisfies assumptions (A1)-(A4). Let Q_C be a projector onto $\ker A_C^T$. The following conditions are equivalent:*

- (i) *system (1) is of index one;*
- (ii) *$\text{rank}(Q_C^T A_{\mathcal{V}}) = n_{\mathcal{V}}$ and $\text{rank}(\begin{bmatrix} A_C & A_{\mathcal{R}} & A_{\mathcal{V}} \end{bmatrix}) = n_{\eta}$;*
- (iii) *$\text{rank}(\begin{bmatrix} A_C & A_{\mathcal{V}} \end{bmatrix}) = \text{rank}(A_C) + n_{\mathcal{V}}$ and $\text{rank}(\begin{bmatrix} A_C & A_{\mathcal{R}} & A_{\mathcal{V}} \end{bmatrix}) = n_{\eta}$.*

Proof. The equivalence of (i) and (ii) was proved in [3]. We now show that the conditions in (ii) and (iii) are equivalent. Obviously, it is enough to prove that $\text{rank}(Q_C^T A_{\mathcal{V}}) = n_{\mathcal{V}}$ if and only if $\text{rank}(\begin{bmatrix} A_C & A_{\mathcal{V}} \end{bmatrix}) = \text{rank}(A_C) + n_{\mathcal{V}}$.

Let $S = \begin{bmatrix} S_1 & S_2 \end{bmatrix}$ be a nonsingular matrix such that the columns of S_2 form a basis of the kernel of A_C^T , i.e., $S_2^T A_C = 0$. Then the projector Q_C can be represented as

$$Q_C = S \begin{bmatrix} 0 & 0 \\ 0 & I \end{bmatrix} S^{-1}.$$

We have $\text{rank}(S_1^T A_C) = \text{rank}(S^T A_C) = \text{rank}(A_C)$ and $\text{rank}(S_2^T A_{\mathcal{V}}) = \text{rank}(Q_C^T A_{\mathcal{V}})$. Therefore,

$$\text{rank}(\begin{bmatrix} A_C & A_{\mathcal{V}} \end{bmatrix}) = \text{rank} \begin{bmatrix} S_1^T A_C & S_1^T A_{\mathcal{V}} \\ 0 & S_2^T A_{\mathcal{V}} \end{bmatrix} = \text{rank}(A_C) + \text{rank}(Q_C^T A_{\mathcal{V}}).$$

Thus, the conditions $\text{rank}(Q_C^T A_{\mathcal{V}}) = n_{\mathcal{V}}$ and $\text{rank}(\begin{bmatrix} A_C & A_{\mathcal{V}} \end{bmatrix}) = \text{rank}(A_C) + n_{\mathcal{V}}$ are equivalent. \square

Remark 2.2 Considering the topological structure of the circuit, the rank conditions in Lemma 2.1 imply that the circuit contains neither *CV*-loops (loops consisting of capacitors and/or voltage sources) except for *C*-loops (loops consisting of capacitors only) nor *LI*-cutsets (cutsets consisting of inductors and/or current sources). \triangleleft

3 Model reduction for nonlinear circuits

In this section, we present a model reduction approach for nonlinear circuits. The first step involves decoupling the nonlinear equations (1) into linear and nonlinear subsystems in a suitable way. Then the linear part is approximated by a reduced-order model of much smaller state space dimension using the PABTEC algorithm [17]. Combining this reduced-order linear model with the unchanged nonlinear subsystem, we obtain a nonlinear reduced-order model that approximates the original system (1). We now describe this model reduction procedure in more detail.

3.1 Decoupling of linear and nonlinear subcircuits

In preparation to the decoupling strategy, we first introduce some notation and present two auxiliary lemmata.

Lemma 3.1 *Let $G_1, G_2 \in \mathbb{R}^{n_{\tilde{x}}, n_{\tilde{x}}}$ be given such that $G_1 + G_2$ is invertible. Then the matrices*

$$\Gamma_{11} = G_1(G_1 + G_2)^{-1}G_1, \quad (2a)$$

$$\Gamma_{12} = G_1(G_1 + G_2)^{-1}G_2, \quad (2b)$$

$$\Gamma_{21} = G_2(G_1 + G_2)^{-1}G_1, \quad (2c)$$

$$\Gamma_{22} = G_2(G_1 + G_2)^{-1}G_2 \quad (2d)$$

satisfy the relations

$$\Gamma_{12} = \Gamma_{21} = G_1 - \Gamma_{11} = G_2 - \Gamma_{22}. \quad (3)$$

Proof. For $\Gamma = G_1 + G_2$, we have

$$\Gamma_{12} = G_1\Gamma^{-1}(G_2 + G_1 - G_1) = G_1 - \Gamma_{11} = G_1 - (G_1 + G_2 - G_2)\Gamma^{-1}G_1 = \Gamma_{21}.$$

Thus, the first two relations in (3) hold. The third relation in (3) can be proved analogously. \square

Lemma 3.2 *Let $A_{\tilde{\mathcal{R}}} \in \{-1, 0, 1\}^{n_{\eta}, n_{\tilde{x}}}$ and let the matrices $G_1, G_2 \in \mathbb{R}^{n_{\tilde{x}}, n_{\tilde{x}}}$ be given such that $\Gamma = G_1 + G_2$ is invertible, and let Γ_{ij} , $i, j = 1, 2$, be as in (2). Then we have the relation*

$$A_{\tilde{\mathcal{R}}}\Gamma_{12}A_{\tilde{\mathcal{R}}}^T = \begin{bmatrix} A_{\tilde{\mathcal{R}}}^1 & A_{\tilde{\mathcal{R}}}^2 \end{bmatrix} \begin{bmatrix} G_1 - \Gamma_{11} & \Gamma_{12} \\ \Gamma_{21} & G_2 - \Gamma_{22} \end{bmatrix} \begin{bmatrix} (A_{\tilde{\mathcal{R}}}^1)^T \\ (A_{\tilde{\mathcal{R}}}^2)^T \end{bmatrix},$$

where $A_{\tilde{\mathcal{R}}}^1 \in \{0, 1\}^{n_{\eta}, n_{\tilde{x}}}$ and $A_{\tilde{\mathcal{R}}}^2 \in \{-1, 0\}^{n_{\eta}, n_{\tilde{x}}}$ satisfy $A_{\tilde{\mathcal{R}}}^1 + A_{\tilde{\mathcal{R}}}^2 = A_{\tilde{\mathcal{R}}}$.

Proof. For

$$A_{\tilde{\mathcal{R}}} = A_{\tilde{\mathcal{R}}}^1 + A_{\tilde{\mathcal{R}}}^2 = \begin{bmatrix} A_{\tilde{\mathcal{R}}}^1 & A_{\tilde{\mathcal{R}}}^2 \end{bmatrix} \begin{bmatrix} I \\ I \end{bmatrix},$$

we get

$$\begin{aligned} A_{\tilde{\mathcal{R}}} \Gamma_{12} A_{\tilde{\mathcal{R}}}^T &= \begin{bmatrix} A_{\tilde{\mathcal{R}}}^1 & A_{\tilde{\mathcal{R}}}^2 \end{bmatrix} \begin{bmatrix} I \\ I \end{bmatrix} \Gamma_{12} \begin{bmatrix} I & I \end{bmatrix} \begin{bmatrix} (A_{\tilde{\mathcal{R}}}^1)^T \\ (A_{\tilde{\mathcal{R}}}^2)^T \end{bmatrix} \\ &= \begin{bmatrix} A_{\tilde{\mathcal{R}}}^1 & A_{\tilde{\mathcal{R}}}^2 \end{bmatrix} \begin{bmatrix} \Gamma_{12} & \Gamma_{12} \\ \Gamma_{12} & \Gamma_{12} \end{bmatrix} \begin{bmatrix} (A_{\tilde{\mathcal{R}}}^1)^T \\ (A_{\tilde{\mathcal{R}}}^2)^T \end{bmatrix}. \end{aligned}$$

Then the statement follows from Lemma 3.1. \square

Definition 3.3 *Two DAE systems*

$$\begin{aligned} \mathcal{E}_1(x_1) \frac{d}{dt} x_1 &= f_1(x_1) + \mathcal{B}_1 u, \\ y_1 &= \mathcal{C}_1 x_1 \end{aligned}$$

and

$$\begin{aligned} \mathcal{E}_2(x_2) \frac{d}{dt} x_2 &= f_2(x_2) + \mathcal{B}_2 u, \\ y_2 &= \mathcal{C}_2 x_2 \end{aligned}$$

with $\mathcal{E}_j(x_j) \in \mathbb{R}^{n,n}$, $f_j(x_j) \in \mathbb{R}^n$, $\mathcal{B}_j \in \mathbb{R}^{n,m}$ and $\mathcal{C}_j \in \mathbb{R}^{p_j,n}$, $j = 1, 2$, are called state equivalent if for a given input u , the solutions of these systems satisfy $x_1 = \Pi x_2$ with a permutation matrix Π .

Our goal is now to extract a linear subcircuit from a nonlinear circuit. This can be achieved, for example, via the replacement of nonlinear circuit devices by controlled current sources. An advantage of this strategy is that no additional nodes and, hence, no additional states are introduced into the system. However, in this case, LI -cutsets may occur that may result in the increasing of the index. To avoid this, we replace the nonlinear capacitors and resistors by controlled voltage sources. Unfortunately, this introduces additional states into the DAE system. Furthermore, the replacement of the nonlinear resistors by voltage sources may lead to the appearance of CV -loops that may again increase the index of the extracted linear DAE system. To overcome this difficulty, we propose to replace the nonlinear resistors by an equivalent circuit consisting of two serial linear resistors and one controlled current source connected parallel to one of the resistors as shown in Figure 2. This introduces additional nodes, but neither additional CV -loops nor LI -cutsets occur in the decoupled subcircuit meaning that the index remains unchanged. The suggested replacements are exemplarily demonstrated in Figure 3, where we present two circuits before and after replacements.

Note that all replacements described above and decoupling the linear subcircuit from the nonlinear circuit can easily be carried out on the netlist level. In the following theorem, we perform this decoupling on the equation level.

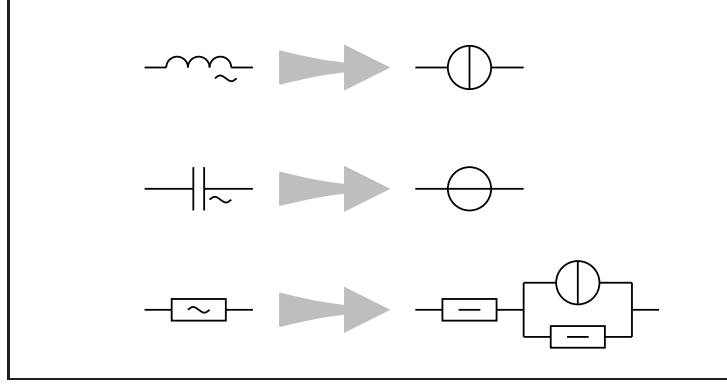


Figure 2: Replacements for nonlinear circuit elements

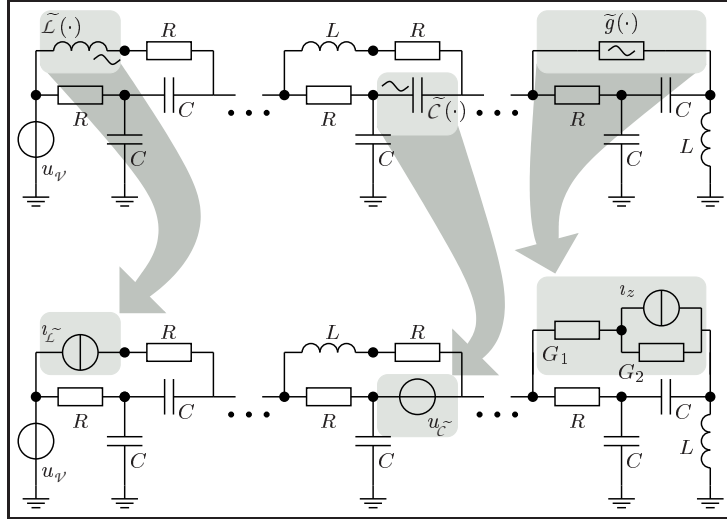


Figure 3: Exemplary replacements

Theorem 3.4 Let $A_{\tilde{\mathcal{R}}}^1 \in \{0, 1\}^{n_\eta, n_{\tilde{\mathcal{R}}}}$ and $A_{\tilde{\mathcal{R}}}^2 \in \{-1, 0\}^{n_\eta, n_{\tilde{\mathcal{R}}}}$ satisfy $A_{\tilde{\mathcal{R}}}^1 + A_{\tilde{\mathcal{R}}}^2 = A_{\tilde{\mathcal{R}}}$, and let $G_1, G_2 \in \mathbb{R}^{n_{\tilde{\mathcal{R}}}, n_{\tilde{\mathcal{R}}}}$ be given such that G_1, G_2 and $\Gamma = G_1 + G_2$ are symmetric, positive definite. Assume that $u_{\tilde{\mathcal{C}}} \in \mathbb{R}^{n_{\tilde{\mathcal{C}}}}$ and $v_z \in \mathbb{R}^{n_{\tilde{\mathcal{R}}}}$ satisfy

$$u_{\tilde{\mathcal{C}}} = A_{\tilde{\mathcal{C}}}^T \eta, \quad (4a)$$

$$v_z = \Gamma G_1^{-1} \tilde{g}(A_{\tilde{\mathcal{R}}}^T \eta) - G_2 A_{\tilde{\mathcal{R}}}^T \eta. \quad (4b)$$

Then system (1) together with the relations

$$v_{\tilde{\mathcal{C}}} = \tilde{\mathcal{C}}(u_{\tilde{\mathcal{C}}}) \frac{d}{dt} u_{\tilde{\mathcal{C}}}, \quad (5a)$$

$$\eta_z = \Gamma^{-1} (G_1 (A_{\tilde{\mathcal{R}}}^1)^T \eta - G_2 (A_{\tilde{\mathcal{R}}}^2)^T \eta - v_z) \quad (5b)$$

for the additional unknowns $\eta_z \in \mathbb{R}^{n_{\tilde{x}}}$ and $v_{\tilde{c}} \in \mathbb{R}^{n_{\tilde{c}}}$ is state equivalent to the system

$$\tilde{\mathcal{L}}(v_{\tilde{c}}) \frac{d}{dt} v_{\tilde{c}} = A_{\tilde{L}}^T \eta \quad (6)$$

coupled with the linear DAE system

$$E \frac{d}{dt} x_\ell = A x_\ell + B u_\ell, \quad (7a)$$

$$y_\ell = B^T x_\ell, \quad (7b)$$

where $x_\ell^T = [\eta^T \ \eta_z^T \mid v_{\tilde{L}}^T \mid v_{\mathcal{V}}^T \ v_{\tilde{c}}^T]$, $u_\ell^T = [v_{\mathcal{J}}^T \ v_z^T \ v_{\tilde{L}}^T \mid u_{\mathcal{V}}^T \ u_{\tilde{c}}^T]$ and

$$E = \begin{bmatrix} A_C C A_C^T & 0 & 0 \\ 0 & L & 0 \\ 0 & 0 & 0 \end{bmatrix}, \quad A = \begin{bmatrix} -A_R G A_R^T & -A_L & -A_V \\ A_L^T & 0 & 0 \\ A_V^T & 0 & 0 \end{bmatrix}, \quad B = \begin{bmatrix} -A_I & 0 \\ 0 & 0 \\ 0 & -I \end{bmatrix}, \quad (7c)$$

with $E, A \in \mathbb{R}^{n_\ell, n_\ell}$, $B \in \mathbb{R}^{n_\ell, m_\ell}$ and the incidence and element matrices

$$A_C = \begin{bmatrix} A_{\tilde{C}} \\ 0 \end{bmatrix}, \quad A_R = \begin{bmatrix} A_{\tilde{\mathcal{R}}} & A_{\tilde{\mathcal{R}}}^1 & A_{\tilde{\mathcal{R}}}^2 \\ 0 & -I & I \end{bmatrix}, \quad A_L = \begin{bmatrix} A_{\tilde{L}} \\ 0 \end{bmatrix}, \quad (7d)$$

$$A_V = \begin{bmatrix} A_{\mathcal{V}} & A_{\tilde{C}} \\ 0 & 0 \end{bmatrix}, \quad A_I = \begin{bmatrix} A_{\mathcal{J}} & A_{\tilde{\mathcal{R}}}^2 & A_{\tilde{L}} \\ 0 & I & 0 \end{bmatrix}, \quad (7e)$$

$$G = \begin{bmatrix} \tilde{\mathcal{G}} & 0 & 0 \\ 0 & G_1 & 0 \\ 0 & 0 & G_2 \end{bmatrix}, \quad C = \tilde{C}, \quad L = \tilde{L}. \quad (7f)$$

Proof. We show that $[x^T \ \eta_z^T \ v_{\tilde{c}}^T]^T$ solves (1) and (5) if and only if $[x_\ell^T \ v_{\tilde{L}}^T]^T$ solves (6) and (7). First note that these vectors are identical up to a permutation. Using (1f), (4a) and the voltage-current relation (5a) for the nonlinear capacitors, we can rewrite system (1a), (1c)-(1f) as

$$A_{\tilde{C}} \tilde{C} A_{\tilde{C}}^T \frac{d}{dt} \eta = -A_{\tilde{\mathcal{R}}} \tilde{\mathcal{G}} A_{\tilde{\mathcal{R}}}^T \eta - A_{\tilde{L}} v_{\tilde{L}} - A_{\mathcal{V}} v_{\mathcal{V}} - A_{\tilde{C}} v_{\tilde{c}} - A_{\mathcal{J}} v_{\mathcal{J}} - A_{\tilde{\mathcal{R}}} \tilde{g}(A_{\tilde{\mathcal{R}}}^T \eta) - A_{\tilde{L}} v_{\tilde{L}}, \quad (8a)$$

$$\tilde{\mathcal{L}} \frac{d}{dt} v_{\tilde{L}} = A_{\tilde{L}}^T \eta, \quad (8b)$$

$$\tilde{\mathcal{L}}(v_{\tilde{c}}) \frac{d}{dt} v_{\tilde{c}} = A_{\tilde{L}}^T \eta, \quad (8c)$$

$$0 = A_{\mathcal{V}}^T \eta - u_{\mathcal{V}}, \quad (8d)$$

$$0 = A_{\tilde{C}}^T \eta - u_{\tilde{c}}. \quad (8e)$$

It follows from (4b) that $\tilde{g}(A_{\tilde{\mathcal{R}}}^T \eta) = G_1 \Gamma^{-1} \iota_z + \Gamma_{12} A_{\tilde{\mathcal{R}}}^T \eta$ with Γ_{12} as in (2b). Substituting this $\tilde{g}(A_{\tilde{\mathcal{R}}}^T \eta)$ in (8a) and inserting the relation (5b) for the variable vector η_z , we have

$$A_{\tilde{\mathcal{C}}} \bar{C} A_{\tilde{\mathcal{C}}}^T \frac{d}{dt} \eta = -(A_{\tilde{\mathcal{R}}} \bar{G} A_{\tilde{\mathcal{R}}}^T + A_{\tilde{\mathcal{R}}} \Gamma_{12} A_{\tilde{\mathcal{R}}}^T) \eta - A_{\tilde{\mathcal{L}}} \iota_{\tilde{\mathcal{L}}} - A_{\mathcal{V}} \iota_{\mathcal{V}} - A_{\tilde{\mathcal{C}}} \iota_{\tilde{\mathcal{C}}} \quad (9a)$$

$$-A_{\mathcal{J}} \iota_{\mathcal{J}} - A_{\tilde{\mathcal{R}}} G_1 \Gamma^{-1} \iota_z - A_{\tilde{\mathcal{L}}} \iota_{\tilde{\mathcal{L}}}$$

$$0 = (G_1 (A_{\tilde{\mathcal{R}}}^1)^T - G_2 (A_{\tilde{\mathcal{R}}}^2)^T) \eta - \Gamma \eta_z - \iota_z, \quad (9b)$$

$$\bar{L} \frac{d}{dt} \iota_{\tilde{\mathcal{L}}} = A_{\tilde{\mathcal{L}}}^T \eta, \quad (9c)$$

$$\tilde{L} (\iota_{\tilde{\mathcal{L}}}) \frac{d}{dt} \iota_{\tilde{\mathcal{L}}} = A_{\tilde{\mathcal{L}}}^T \eta, \quad (9d)$$

$$0 = A_{\mathcal{V}}^T \eta - u_{\mathcal{V}}, \quad (9e)$$

$$0 = A_{\tilde{\mathcal{C}}}^T \eta - u_{\tilde{\mathcal{C}}}. \quad (9f)$$

Finally, multiplying (9b) by $-(A_{\tilde{\mathcal{R}}}^1 G_1 - A_{\tilde{\mathcal{R}}}^2 G_2) \Gamma^{-1}$ and adding up the resulting equation to (9a), we obtain using Lemma 3.1 the system

$$A_{\tilde{\mathcal{C}}} \bar{C} A_{\tilde{\mathcal{C}}}^T \frac{d}{dt} \eta = -(A_{\tilde{\mathcal{R}}} \bar{G} A_{\tilde{\mathcal{R}}}^T + A_{\tilde{\mathcal{R}}}^1 G_1 (A_{\tilde{\mathcal{R}}}^1)^T + A_{\tilde{\mathcal{R}}}^2 G_2 (A_{\tilde{\mathcal{R}}}^2)^T) \eta \quad (10a)$$

$$+ (A_{\tilde{\mathcal{R}}}^1 G_1^T - A_{\tilde{\mathcal{R}}}^2 G_2^T) \eta_z - A_{\tilde{\mathcal{L}}} \iota_{\tilde{\mathcal{L}}} - A_{\mathcal{V}} \iota_{\mathcal{V}} - A_{\tilde{\mathcal{C}}} \iota_{\tilde{\mathcal{C}}}$$

$$-A_{\mathcal{J}} \iota_{\mathcal{J}} - A_{\tilde{\mathcal{R}}}^2 \iota_z - A_{\tilde{\mathcal{L}}} \iota_{\tilde{\mathcal{L}}},$$

$$0 = (G_1 (A_{\tilde{\mathcal{R}}}^1)^T - G_2 (A_{\tilde{\mathcal{R}}}^2)^T) \eta - \Gamma \eta_z - \iota_z, \quad (10b)$$

$$\bar{L} \frac{d}{dt} \iota_{\tilde{\mathcal{L}}} = A_{\tilde{\mathcal{L}}}^T \eta, \quad (10c)$$

$$\tilde{L} (\iota_{\tilde{\mathcal{L}}}) \frac{d}{dt} \iota_{\tilde{\mathcal{L}}} = A_{\tilde{\mathcal{L}}}^T \eta, \quad (10d)$$

$$0 = A_{\mathcal{V}}^T \eta - u_{\mathcal{V}}, \quad (10e)$$

$$0 = A_{\tilde{\mathcal{C}}}^T \eta - u_{\tilde{\mathcal{C}}}. \quad (10f)$$

Thus, equations (10), (1b) are state equivalent to the DAE system (6), (7). \square

Note that the system matrices in the decoupled linear system (7) are in the MNA form with $A_C \in \mathbb{R}^{n_{\tilde{\eta}}, n_C}$, $A_L \in \mathbb{R}^{n_{\tilde{\eta}}, n_L}$, $A_R \in \mathbb{R}^{n_{\tilde{\eta}}, n_R}$, $A_V \in \mathbb{R}^{n_{\tilde{\eta}}, n_V}$, $A_I \in \mathbb{R}^{n_{\tilde{\eta}}, n_I}$ and $G \in \mathbb{R}^{n_R, n_R}$, $C \in \mathbb{R}^{n_C, n_C}$, $L \in \mathbb{R}^{n_L, n_L}$, where $n_{\tilde{\eta}} = n_{\eta} + n_{\tilde{\mathcal{R}}}$, $n_C = n_{\tilde{\mathcal{C}}}$, $n_L = n_{\tilde{\mathcal{L}}}$, $n_R = n_{\tilde{\mathcal{R}}} + 2n_{\tilde{\mathcal{R}}}$, $n_V = n_{\mathcal{V}} + n_{\tilde{\mathcal{C}}}$ and $n_I = n_{\mathcal{J}} + n_{\tilde{\mathcal{R}}} + n_{\tilde{\mathcal{L}}}$. System (7) has the state space dimension $n_{\ell} = n_{\tilde{\eta}} + n_L + n_V$ and the input space dimension $m_{\ell} = n_I + n_V$. It should also be noted that the state equivalence in Theorem 3.4 is independent of the choice of the matrices G_1 and G_2 satisfying the assumptions in the theorem. The substitution of nonlinear resistors with equivalent circuits as described above implies that these matrices are diagonal and their diagonal elements are conductances of the first and the second linear resistors, respectively, in the replacement circuits. The following example demonstrates that these conductances can indeed be chosen arbitrarily.

Example 3.5 Consider a simple RCV circuit shown in Figure 4a. Such a circuit can be

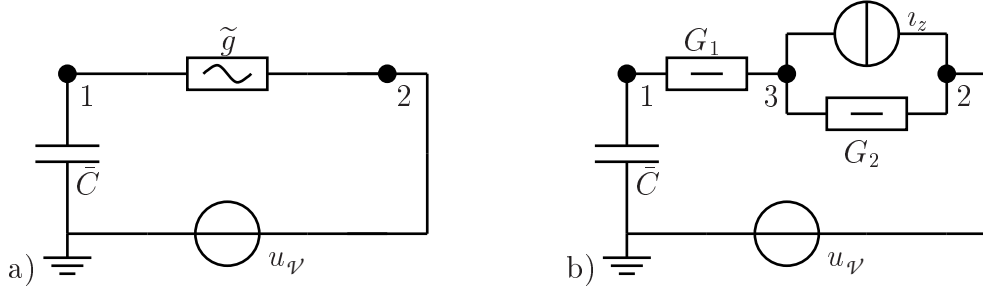


Figure 4: Simple RCV circuit

described by the MNA equations in the form

$$\begin{bmatrix} \bar{C} & 0 & 0 \\ 0 & 0 & 0 \\ 0 & 0 & 0 \end{bmatrix} \begin{bmatrix} \frac{d}{dt}\eta_1 \\ \frac{d}{dt}\eta_2 \\ \frac{d}{dt}i_{\mathcal{V}} \end{bmatrix} = \begin{bmatrix} 0 & 0 & 0 \\ 0 & 0 & 1 \\ 0 & -1 & 0 \end{bmatrix} \begin{bmatrix} \eta_1 \\ \eta_2 \\ i_{\mathcal{V}} \end{bmatrix} + \begin{bmatrix} -\tilde{g}(\eta_1 - \eta_2) \\ \tilde{g}(\eta_1 - \eta_2) \\ 0 \end{bmatrix} + \begin{bmatrix} 0 \\ 0 \\ -1 \end{bmatrix} u_{\mathcal{V}}, \quad (11a)$$

$$y = \begin{bmatrix} 0 & 0 & -1 \end{bmatrix} \begin{bmatrix} \eta_1 \\ \eta_2 \\ i_{\mathcal{V}} \end{bmatrix}. \quad (11b)$$

The incidence matrices are given by

$$A_{\bar{C}} = \begin{bmatrix} 1 \\ 0 \end{bmatrix}, \quad A_{\tilde{\mathcal{R}}} = \begin{bmatrix} 1 \\ -1 \end{bmatrix}, \quad A_{\mathcal{V}} = \begin{bmatrix} 0 \\ -1 \end{bmatrix},$$

and, hence,

$$A_{\tilde{\mathcal{R}}}^1 = \begin{bmatrix} 1 \\ 0 \end{bmatrix}, \quad A_{\tilde{\mathcal{R}}}^2 = \begin{bmatrix} 0 \\ -1 \end{bmatrix}.$$

According to the developed replacement strategy, we introduce the new node 3 with the potential η_3 , two linear resistors with conductances G_1 and G_2 and the current source

$$i_z = \Gamma G_1^{-1} \tilde{g}(\eta_1 - \eta_2) - G_2(\eta_1 - \eta_2) \quad (12)$$

with $\Gamma = G_1 + G_2$. The new circuit is shown in Figure 4b. It is described by the MNA system

$$\begin{bmatrix} \bar{C} & 0 & 0 & 0 \\ 0 & 0 & 0 & 0 \\ 0 & 0 & 0 & 0 \\ 0 & 0 & 0 & 0 \end{bmatrix} \begin{bmatrix} \frac{d}{dt}\eta_1 \\ \frac{d}{dt}\eta_2 \\ \frac{d}{dt}\eta_3 \\ \frac{d}{dt}i_{\mathcal{V}} \end{bmatrix} = \begin{bmatrix} -G_1 & 0 & G_1 & 0 \\ 0 & -G_2 & G_2 & 1 \\ G_1 & G_2 & -\Gamma & 0 \\ 0 & -1 & 0 & 0 \end{bmatrix} \begin{bmatrix} \eta_1 \\ \eta_2 \\ \eta_3 \\ i_{\mathcal{V}} \end{bmatrix} + \begin{bmatrix} 0 & 0 \\ 1 & 0 \\ -1 & 0 \\ 0 & -1 \end{bmatrix} \begin{bmatrix} i_z \\ u_{\mathcal{V}} \end{bmatrix}, \quad (13a)$$

$$y_{\ell} = \begin{bmatrix} 0 & 1 & -1 & 0 \\ 0 & 0 & 0 & -1 \end{bmatrix} \begin{bmatrix} \eta_1 \\ \eta_2 \\ \eta_3 \\ i_{\mathcal{V}} \end{bmatrix}. \quad (13b)$$

We now show that system (11a) together with the equation

$$\eta_3 = \Gamma^{-1}(G_1\eta_1 + G_2\eta_2 - \iota_z) \quad (14)$$

is equivalent to (13a) independent of the choice of G_1 and G_2 . Indeed, the third equation in (13a) yields (14). Substituting η_3 in the first and the second equations in (13a) and taking into account (12), we obtain

$$\begin{aligned} \begin{bmatrix} \bar{C} & 0 & 0 \\ 0 & 0 & 0 \\ 0 & 0 & 0 \end{bmatrix} \begin{bmatrix} \frac{d}{dt}\eta_1 \\ \frac{d}{dt}\eta_2 \\ \frac{d}{dt}\iota_{\mathcal{V}} \end{bmatrix} &= \begin{bmatrix} -G_1\eta_1 + G_1\Gamma^{-1}(G_1\eta_1 + G_2\eta_2 - \iota_z) \\ -G_2\eta_2 + G_2\Gamma^{-1}(G_1\eta_1 + G_2\eta_2 - \iota_z) + \iota_z + \iota_{\mathcal{V}} \\ -\eta_2 - u_{\mathcal{V}} \end{bmatrix} \\ &= \begin{bmatrix} -\tilde{g}(\eta_1 - \eta_2) \\ \tilde{g}(\eta_1 - \eta_2) + \iota_{\mathcal{V}} \\ -\eta_2 - u_{\mathcal{V}} \end{bmatrix}. \end{aligned}$$

The reverse statement can be proved analogously. \triangleleft

The following theorem establishes the well-posedness of the decoupled linear system (7) under conditions that the original circuit does not contain $\tilde{C}V$ -loops (loops consisting of nonlinear resistors and/or voltage sources) and $\tilde{L}I$ -cutsets (cutsets consisting of nonlinear inductors and/or current sources). $\tilde{C}V$ -loops and $\tilde{L}I$ -cutsets in the original circuit (1) would lead after the replacement of the nonlinear capacitors and nonlinear inductors by voltage sources and current sources, respectively, to V -loops and I -cutsets in the decoupled circuit (7) that would violate its well-posedness.

Theorem 3.6 *Let a nonlinear circuit satisfy assumptions (A1)-(A4). Additionally, assume that it contains neither $\tilde{C}V$ -loops nor $\tilde{L}I$ -cutsets. Then the linear DAE system (7) modeling the extracted linear subcircuit is well-posed in the sense that*

1. *the matrix A_V has full column rank,*
2. *the matrix $[A_C \ A_L \ A_R \ A_V]$ has full row rank,*
3. *the matrices C , L and G are symmetric and positive definite.*

Proof. The third property immediately follows from assumptions (A3), (A4) and the diagonal structure of G_1 and G_2 . If the circuit does not contain $\tilde{C}V$ -loops, then the matrix $[A_{\mathcal{V}} \ A_{\tilde{C}}]$ has full column rank. Hence, A_V in (7e) has also full column rank. The absence of $\tilde{L}I$ -cutsets implies that the matrix $[A_{\tilde{C}} \ A_{\tilde{C}} \ A_{\tilde{L}} \ A_{\tilde{\mathcal{R}}} \ A_{\tilde{\mathcal{R}}} \ A_{\mathcal{V}}]$ has full row rank. Then it follows from

$$\begin{aligned} \text{rank}([A_C \ A_L \ A_R \ A_V]) &= \text{rank}\left(\begin{bmatrix} A_{\tilde{C}} & A_{\tilde{L}} & A_{\tilde{\mathcal{R}}} & A_{\tilde{\mathcal{R}}}^1 & A_{\tilde{\mathcal{R}}}^2 & A_{\mathcal{V}} & A_{\tilde{C}} \\ 0 & 0 & 0 & -I & I & 0 & 0 \end{bmatrix}\right) \\ &= \text{rank}\left(\begin{bmatrix} A_{\tilde{C}} & A_{\tilde{C}} & A_{\tilde{L}} & A_{\tilde{\mathcal{R}}} & A_{\tilde{\mathcal{R}}} & A_{\mathcal{V}} & 0 \\ 0 & 0 & 0 & 0 & 0 & 0 & I \end{bmatrix}\right) \end{aligned}$$

that the matrix $\begin{bmatrix} A_C & A_L & A_R & A_V \end{bmatrix}$ has also full row rank. \square

We now show that the slightly stronger index one condition for the nonlinear circuit guarantees that the decoupled linear DAE system (7) is well-posed and, in addition, has index at most one.

Theorem 3.7 *Let a nonlinear circuit satisfy assumptions (A1)-(A4). If this circuit contains neither CV-loops except for \bar{C} -loops with linear capacitors nor LI-cutsets, then the linear DAE system (7) modeling the extracted linear subcircuit is well-posed and is of index at most one.*

Proof. Since the circuit does not have LI-cutsets and CV-loops except for \bar{C} -loops, Theorem 3.6 implies that system (7) is well-posed. Moreover, from Remark 2.2 we have

$$\begin{aligned} \text{rank}(\begin{bmatrix} A_{\bar{C}} & A_{\bar{C}} & A_{\mathcal{V}} \end{bmatrix}) &= \text{rank}(A_{\bar{C}}) + n_{\bar{C}} + n_{\mathcal{V}}, \\ \text{rank}(\begin{bmatrix} A_{\bar{C}} & A_{\bar{C}} & A_{\bar{\mathcal{R}}} & A_{\bar{\mathcal{R}}} & A_{\mathcal{V}} \end{bmatrix}) &= n_{\bar{\eta}}. \end{aligned}$$

Therefore,

$$\begin{aligned} \text{rank}(\begin{bmatrix} A_C & A_V \end{bmatrix}) &= \text{rank}(\begin{bmatrix} A_{\bar{C}} & A_{\mathcal{V}} & A_{\bar{C}} \end{bmatrix}) = \text{rank}(A_{\bar{C}}) + (n_{\mathcal{V}} + n_{\bar{C}}) = \text{rank}(A_C) + n_V, \\ \text{rank}[A_C, A_R, A_V] &= \text{rank}\left(\begin{bmatrix} A_{\bar{C}} & A_{\bar{\mathcal{R}}} & A_{\bar{\mathcal{R}}} & A_{\mathcal{V}} & A_{\bar{C}} & 0 \\ 0 & 0 & 0 & 0 & 0 & I \end{bmatrix}\right) = n_{\bar{\eta}} + n_{\bar{\mathcal{R}}} = n_{\bar{\eta}}. \end{aligned}$$

Note that $n_{\bar{\eta}} = n_{\bar{\eta}} + n_{\bar{\mathcal{R}}}$ is the number of nodes in (7). Thus, from Lemma 2.1 we get that the system (7) is of index at most one. \square

Note that the index one condition for system (7) implies that its transfer function is proper, i.e., it is bounded at infinity. The approximation of such systems is much easier than that of systems with an improper transfer function [21].

3.2 Balancing-related model reduction of linear circuits

We now aim to approximate the decoupled linear DAE system (7) by a reduced-order model

$$\begin{aligned} \hat{E} \frac{d}{dt} \hat{x}_\ell &= \hat{A} \hat{x}_\ell + \hat{B} u, \\ \hat{y}_\ell &= \hat{C} \hat{x}_\ell, \end{aligned} \tag{15}$$

where $\hat{E}, \hat{A} \in \mathbb{R}^{r_\ell, r_\ell}$, $\hat{B} \in \mathbb{R}^{r_\ell, m_\ell}$, $\hat{C} \in \mathbb{R}^{m_\ell, r_\ell}$, and r_ℓ is much smaller than the state space dimension n_ℓ of system (7). Such a model can be computed via the PABTEC algorithm [17] based on balanced truncation. In general, balanced truncation model reduction methods rely on the transformation of the dynamical system into a balanced form whose controllability and observability Gramians are both equal to a diagonal matrix. Then a reduced-order model is determined by the truncation of the states corresponding to small diagonal elements of the balanced Gramians. Depending on system properties, different types of

Gramians may be introduced. For passivity-preserving model reduction, the Gramians are defined as unique stabilizing solutions of the projected Riccati equations

$$EX\check{A}^T + \check{A}XE^T + EX\check{C}^T\check{C}XE^T + P_l\check{B}\check{B}^T P_l^T = 0, \quad X = P_r X P_r^T, \quad (16)$$

$$E^T Y \check{A} + \check{A}^T Y E + E^T Y \check{B}\check{B}^T Y E + P_r^T \check{C}^T \check{C} P_r = 0, \quad Y = P_l^T Y P_l, \quad (17)$$

where

$$\begin{aligned} \check{A} &= A - BB^T - 2P_l B(I - M_0^T M_0)^{-1} M_0^T B^T P_r, \\ \check{B} &= \sqrt{2} B J_o^{-1}, \quad \check{C} = \sqrt{2} J_c^{-1} B^T, \\ J_o^T J_o &= I - M_0^T M_0, \quad J_c J_c^T = I - M_0 M_0^T, \\ M_0 &= I - \lim_{s \rightarrow \infty} B^T (sE - A + BB^T)^{-1} B, \end{aligned}$$

and P_r and P_l are the spectral projectors onto the right and left deflating subspaces of the pencil $\lambda E - (A - BB^T)$ corresponding to the finite eigenvalues.

Let R_X and R_Y be the Cholesky factors of the Gramians $X = R_X R_X^T$ and $Y = R_Y R_Y^T$, respectively. Compute the singular value decomposition

$$R_Y^T E R_X = [U_1, U_2] \begin{bmatrix} \Pi_1 & 0 \\ 0 & \Pi_2 \end{bmatrix} [V_1, V_2]^T,$$

where $[U_1, U_2]$ and $[V_1, V_2]$ have orthonormal columns,

$$\Pi_1 = \text{diag}(\pi_1, \dots, \pi_r), \quad \Pi_2 = \text{diag}(\pi_{r+1}, \dots, \pi_q)$$

with $\pi_1 \geq \dots \geq \pi_r > \pi_{r+1} \geq \dots \geq \pi_q$. The values π_j are called the *characteristic values* of system (7). They determine the important state variables of the balanced system. The reduced-order model (15) can be computed by projection onto the left and right subspaces corresponding to the dominant characteristic values. Such a model is given by

$$\begin{aligned} \hat{E} &= \begin{bmatrix} I_r & 0 \\ 0 & 0 \end{bmatrix}, \quad \hat{A} = \frac{1}{2} \begin{bmatrix} 2W^T A T & \sqrt{2} W^T B C_\infty \\ -\sqrt{2} B_\infty B^T T & 2I - B_\infty C_\infty \end{bmatrix}, \\ \hat{B} &= \begin{bmatrix} W^T B \\ -B_\infty / \sqrt{2} \end{bmatrix}, \quad \hat{C} = [B^T T \quad C_\infty / \sqrt{2}], \end{aligned} \quad (18)$$

where $W = L U_1 \Pi_1^{-1/2}$, $T = R V_1 \Pi_1^{-1/2}$, and the matrices B_∞ and C_∞ are chosen such that $I - M_0 = C_\infty B_\infty$. One can show that the reduced-order system (15), (18) is passive, reciprocal and its index does not exceed the index of (7), see [17]. Let

$$\mathbf{G}(s) = B^T (sE - A)^{-1} B, \quad \hat{\mathbf{G}}(s) = \hat{C} (s\hat{E} - \hat{A})^{-1} \hat{B}$$

be the transfer functions of systems (7) and (15), respectively. Then we can estimate the \mathbb{H}_∞ -norm of the error defined as

$$\|\hat{\mathbf{G}} - \mathbf{G}\|_{\mathbb{H}_\infty} = \sup_{\omega \in \mathbb{R}} \|\hat{\mathbf{G}}(i\omega) - \mathbf{G}(i\omega)\|,$$

where $\|\cdot\|$ denotes the spectral matrix norm. If $\|I + \mathbf{G}\|_{\mathbb{H}_\infty} (\pi_{r+1} + \dots + \pi_q) < 2$, then we have the following error bound

$$\|\hat{\mathbf{G}} - \mathbf{G}\|_{\mathbb{H}_\infty} \leq 2\|I + \mathbf{G}\|_{\mathbb{H}_\infty}^2 (\pi_{r+1} + \dots + \pi_q), \quad (19)$$

see [16]. In the time domain, the error in the output can be bounded as

$$\|\hat{y}_\ell - y_\ell\|_{\mathbb{L}_2} \leq \|\hat{\mathbf{G}} - \mathbf{G}\|_{\mathbb{H}_\infty} \|u\|_{\mathbb{L}_2}. \quad (20)$$

By exploiting the structure of circuit equations, this model reduction procedure can be made more efficient and accurate. Since the MNA matrices in (7c) satisfy

$$E^T = S_{\text{int}} E S_{\text{int}}, \quad A^T = S_{\text{int}} A S_{\text{int}}, \quad B^T = S_{\text{ext}} B^T S_{\text{int}},$$

where $S_{\text{int}} = \text{diag}(I_{n_{\bar{n}}}, -I_{n_L}, -I_{n_V})$ and $S_{\text{ext}} = \text{diag}(I_{n_I}, -I_{n_V})$, we find that

$$P_l = S_{\text{int}} P_r^T S_{\text{int}}, \quad Y_{\text{min}} = S_{\text{int}} X_{\text{min}} S_{\text{int}} = S_{\text{int}} R_X R_X^T S_{\text{int}}^T = R_Y R_Y^T.$$

Thus, for the linear circuit equations (7), it is enough to compute one projector and solve one projected Riccati equation only. Another projector and also the solution of the dual Riccati equation are given for free. Furthermore, we can show that $R_Y^T E R_X = R_X^T S_{\text{int}} E R_X$ is symmetric. Then the characteristic values π_j can be computed from an eigenvalue decomposition of $R_X^T S_{\text{int}} E R_X$ instead of a more expensive singular value decomposition. If λ_j are eigenvalues of $R_X^T S_{\text{int}} E R_X$, then $\pi_j = |\lambda_j|$. Finally, using the symmetry of the matrix $(I - M_0)S_{\text{ext}}$, we can determine B_∞ and C_∞ from the eigenvalue decomposition of $(I - M_0)S_{\text{ext}}$. The resulting model reduction method is summarized in Algorithm 3.2. Note that for RC and RL circuits, also the passivity-preserving balanced truncation model reduction approach based on projected Lyapunov equations [18] can be applied to compute the reduced-order model (15).

3.3 Reduced-order nonlinear circuit

We now apply the PABTEC method to the linear descriptor system (7). As a result we obtain a reduced-order model (15). In particular, this model has the form

$$\hat{E} \frac{d}{dt} \hat{x}_\ell = \hat{A} \hat{x}_\ell + \begin{bmatrix} \hat{B}_1 & \hat{B}_2 & \hat{B}_3 & \hat{B}_4 & \hat{B}_5 \end{bmatrix} \begin{bmatrix} v_{\mathcal{J}} \\ v_z \\ v_{\bar{\mathcal{L}}} \\ u_{\mathcal{V}} \\ u_{\bar{\mathcal{C}}} \end{bmatrix}, \quad (21a)$$

$$\begin{bmatrix} \hat{y}_{\ell 1} \\ \hat{y}_{\ell 2} \\ \hat{y}_{\ell 3} \\ \hat{y}_{\ell 4} \\ \hat{y}_{\ell 5} \end{bmatrix} = \begin{bmatrix} \hat{C}_1 \\ \hat{C}_2 \\ \hat{C}_3 \\ \hat{C}_4 \\ \hat{C}_5 \end{bmatrix} \hat{x}_\ell, \quad (21b)$$

Algorithm 1 Passivity-preserving balanced truncation for electrical circuits (PABTEC).

Given (E, A, B, B^T) as in (7c), compute a reduced-order model $(\hat{E}, \hat{A}, \hat{B}, \hat{C})$.

1. Compute the Cholesky factor R_X of $X = R_X R_X^T$ that is the stabilizing solution of the projected Riccati equation (16).
2. Compute the eigenvalue decomposition

$$R_X^T S_{\text{int}} E R_X = [U_1, U_2] \begin{bmatrix} \Lambda_1 & 0 \\ 0 & \Lambda_2 \end{bmatrix} [U_1, U_2]^T,$$

where $[U_1, U_2]$ is orthogonal, $\Lambda_1 = \text{diag}(\lambda_1, \dots, \lambda_r)$ and $\Lambda_2 = \text{diag}(\lambda_{r+1}, \dots, \lambda_q)$.

3. Compute the eigenvalue decomposition $(I - M_0)S_{\text{ext}} = U_0 \Lambda_0 U_0^T$, where U_0 is orthogonal and $\Lambda_0 = \text{diag}(\hat{\lambda}_1, \dots, \hat{\lambda}_{m_\ell})$.
4. Compute the reduced-order system (18), where

$$\begin{aligned} B_\infty &= S_0 |\Lambda_0|^{1/2} U_0^T S_{\text{ext}}, & C_\infty &= U_0 |\Lambda_0|^{1/2}, & S_0 &= \text{sign}(\Lambda_0), \\ W &= L U_1 |\Lambda_1|^{-1/2}, & T &= S_{\text{int}} L U_1 S_1 |\Lambda_1|^{-1/2}, & S_1 &= \text{sign}(\Lambda_1), \\ |\Lambda_0| &= \text{diag}(|\hat{\lambda}_1|, \dots, |\hat{\lambda}_{m_\ell}|), & |\Lambda_1| &= \text{diag}(|\lambda_1|, \dots, |\lambda_r|). \end{aligned}$$

where $\hat{y}_{\ell j} = \hat{C}_j \hat{x}_\ell$, $j = 1, \dots, 5$, approximate the corresponding components of the output y_ℓ in (7a). Therefore, we have

$$-(A_{\mathcal{R}}^2)^T \eta - \eta_z \approx \hat{C}_2 \hat{x}_\ell, \quad (22a)$$

$$-A_{\mathcal{L}}^T \eta \approx \hat{C}_3 \hat{x}_\ell, \quad (22b)$$

$$-\iota_{\tilde{z}} \approx \hat{C}_5 \hat{x}_\ell. \quad (22c)$$

Then the nonlinear systems (5a) and (6) are approximated by

$$\tilde{\mathcal{C}}(\hat{u}_{\tilde{z}}) \frac{d}{dt} \hat{u}_{\tilde{z}} = -\hat{C}_5 \hat{x}_\ell \quad (23)$$

and

$$\tilde{\mathcal{L}}(\hat{\iota}_{\tilde{z}}) \frac{d}{dt} \hat{\iota}_{\tilde{z}} = -\hat{C}_3 \hat{x}_\ell, \quad (24)$$

respectively. Here, $\hat{u}_{\tilde{z}}$ and $\hat{\iota}_{\tilde{z}}$ form approximations to $u_{\tilde{z}}$ and $\iota_{\tilde{z}}$, respectively. Furthermore, for η_z defined in (5b) and ι_z defined in (4b), we have

$$\begin{aligned} -(A_{\mathcal{R}}^2)^T \eta - \eta_z &= -(A_{\mathcal{R}}^2)^T \eta - \Gamma^{-1} (G_1 (A_{\mathcal{R}}^1)^T - G_2 (A_{\mathcal{R}}^2)^T) \eta + \Gamma^{-1} \iota_z \\ &= -(A_{\mathcal{R}}^2)^T \eta - \Gamma^{-1} G_1 (A_{\mathcal{R}}^1 + A_{\mathcal{R}}^2)^T \eta + (A_{\mathcal{R}}^2)^T \eta + \Gamma^{-1} \iota_z \\ &= -\Gamma^{-1} G_1 A_{\mathcal{R}}^T \eta + \Gamma^{-1} \iota_z \\ &= -\Gamma^{-1} G_1 A_{\mathcal{R}}^T \eta + G_1^{-1} \tilde{g}(A_{\mathcal{R}}^T \eta) - \Gamma^{-1} G_2 A_{\mathcal{R}}^T \eta \\ &= -A_{\mathcal{R}}^T \eta + G_1^{-1} \tilde{g}(A_{\mathcal{R}}^T \eta). \end{aligned}$$

Taking into account (22a), the vector $u_{\tilde{\mathcal{R}}} = A_{\tilde{\mathcal{R}}}^T \eta$ can be approximated by $\hat{u}_{\tilde{\mathcal{R}}}$ satisfying

$$0 = -G_1 \hat{C}_2 \hat{x}_\ell - G_1 \hat{u}_{\tilde{\mathcal{R}}} + \tilde{g}(\hat{u}_{\tilde{\mathcal{R}}}). \quad (25)$$

Combining (21), (23), (24), (25) and $i_z \approx \Gamma G_1^{-1} \tilde{g}(\hat{u}_{\tilde{\mathcal{R}}}) - G_2 \hat{u}_{\tilde{\mathcal{R}}}$, we obtain the DAE system

$$\begin{aligned} \hat{E} \frac{d}{dt} \hat{x}_\ell &= \hat{A} \hat{x}_\ell + \hat{B}_3 \hat{i}_{\tilde{\mathcal{L}}} + \hat{B}_5 \hat{u}_{\tilde{\mathcal{C}}} - \hat{B}_2 G_2 \hat{u}_{\tilde{\mathcal{R}}} + \hat{B}_2 \Gamma G_1^{-1} \tilde{g}(\hat{u}_{\tilde{\mathcal{R}}}) + \hat{B}_1 u_{\mathcal{J}} + \hat{B}_4 u_{\mathcal{V}}, \\ \tilde{\mathcal{L}}(\hat{i}_{\tilde{\mathcal{L}}}) \frac{d}{dt} \hat{i}_{\tilde{\mathcal{L}}} &= -\hat{C}_3 \hat{x}_\ell, \\ \tilde{\mathcal{C}}(\hat{u}_{\tilde{\mathcal{C}}}) \frac{d}{dt} \hat{u}_{\tilde{\mathcal{C}}} &= -\hat{C}_5 \hat{x}_\ell, \\ 0 &= -G_1 \hat{C}_2 \hat{x}_\ell - G_1 \hat{u}_{\tilde{\mathcal{R}}} + \tilde{g}(\hat{u}_{\tilde{\mathcal{R}}}). \end{aligned}$$

Finally, multiplying the last equation by $-\hat{B}_2 \Gamma G_1^{-1}$ and adding up the resulting equation to the first one, we obtain the reduced-order nonlinear model

$$\begin{aligned} \hat{\mathcal{E}}(\hat{x}) \frac{d}{dt} \hat{x} &= \hat{\mathcal{A}} \hat{x} + \hat{f}(\hat{x}) + \hat{\mathcal{B}} u, \\ \hat{y} &= \hat{\mathcal{C}} \hat{x}, \end{aligned} \quad (26a)$$

where $\hat{x}^T = \begin{bmatrix} \hat{x}_\ell^T & \hat{i}_{\tilde{\mathcal{L}}}^T & \hat{u}_{\tilde{\mathcal{C}}}^T & \hat{u}_{\tilde{\mathcal{R}}}^T \end{bmatrix}$, $u^T = \begin{bmatrix} u_{\mathcal{J}}^T & u_{\mathcal{V}}^T \end{bmatrix}$ and

$$\hat{\mathcal{E}}(\hat{x}) = \begin{bmatrix} \hat{E} & 0 & 0 & 0 \\ 0 & \tilde{\mathcal{L}}(\hat{i}_{\tilde{\mathcal{L}}}) & 0 & 0 \\ 0 & 0 & \tilde{\mathcal{C}}(\hat{u}_{\tilde{\mathcal{C}}}) & 0 \\ 0 & 0 & 0 & 0 \end{bmatrix}, \quad \hat{\mathcal{A}} = \begin{bmatrix} \hat{A} + \hat{B}_2 \Gamma \hat{C}_2 & \hat{B}_3 & \hat{B}_5 & \hat{B}_2 G_1 \\ -\hat{C}_3 & 0 & 0 & 0 \\ -\hat{C}_5 & 0 & 0 & 0 \\ -G_1 \hat{C}_2 & 0 & 0 & -G_1 \end{bmatrix}, \quad (26b)$$

$$\hat{f}(\hat{x}) = \begin{bmatrix} 0 \\ 0 \\ 0 \\ \tilde{g}(\hat{u}_{\tilde{\mathcal{R}}}) \end{bmatrix}, \quad \hat{\mathcal{B}} = \begin{bmatrix} \hat{B}_1 & \hat{B}_4 \\ 0 & 0 \\ 0 & 0 \\ 0 & 0 \end{bmatrix}, \quad \hat{\mathcal{C}} = \begin{bmatrix} \hat{C}_1 & 0 & 0 & 0 \\ \hat{C}_4 & 0 & 0 & 0 \end{bmatrix}. \quad (26c)$$

This model represents a nonlinear approximation to the nonlinear DAE system (1). It can now be used for further investigations in steady-state analysis, transient analysis or sensitivity analysis of electronic circuits. Note that the error bounds (19), (20) for the reduced-order linear subsystem (21) can be used to estimate the error in the output of the reduced-order nonlinear system (26), see [9] for such estimates for a special class of nonlinear circuits. Error bounds for general circuits remain for future work.

4 Numerical Experiments

In this section, we present some results of numerical experiments for two different nonlinear circuits. The computations were done with MATLAB.

Example 4.1 First, we consider a nonlinear circuit shown in Figure 5. It contains 1501 linear capacitors, 1500 linear resistors, 1 voltage source and 1 diode. Such a circuit is described by the DAE system (1) of the state space dimension $n = 1503$. We simulate this system on the time interval $\mathbb{I} = [0\text{s}, 0.07\text{s}]$ with a fixed stepsize 10^{-5}s using the BDF method of order 2. The voltage source is given by $u_{\nu}(t) = 10 \sin(100\pi t)^4 \text{ V}$, see Figure 6. The linear resistors have the same resistance $R = 2 \text{ k}\Omega$, the linear capacitors have the same capacitance $C = 0.02 \mu\text{F}$ and the diode has a characteristic curve $g(u_{\tilde{x}}) = 10^{-14}(\exp(40\frac{1}{\sqrt{V}}u_{\tilde{x}}) - 1) \text{ A}$.

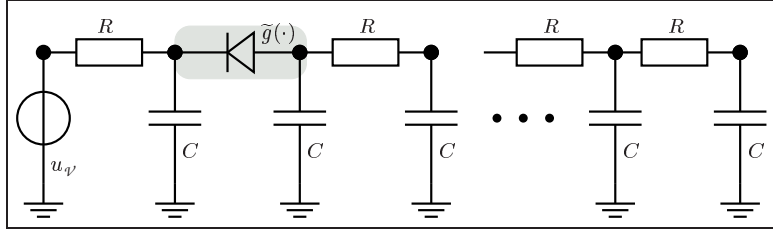


Figure 5: Nonlinear RC circuit

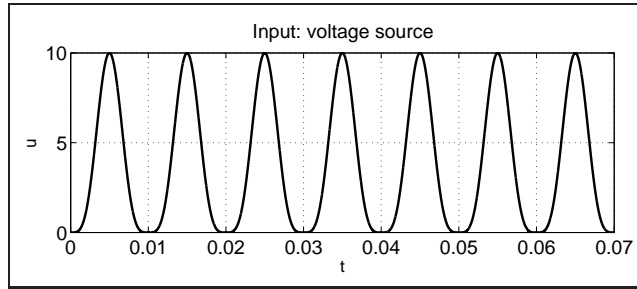


Figure 6: Voltage source for the RC circuit

The dimension r_ℓ of the reduced-order linear system (15) was determined as $r_\ell = r + r_0$, where $r_0 = \text{rank}(I - M_0)$ and r satisfies the condition $(\pi_{r+1} + \dots + \pi_q) < \text{tol}$ with a prescribed tolerance tol . For comparison, we compute the reduced-order linear models for the different tolerances $\text{tol} = 10^{-2}, 10^{-3}, 10^{-4}, 10^{-5}$. The numerical results are given in Figure 7. In the upper plot of each subfigure, we present the computed outputs $y(t) = -v_{\nu}(t)$ and $\hat{y}(t)$ of the original and reduced-order nonlinear systems, respectively, whereas the lower plot shows the error $|\hat{y}(t) - y(t)|$.

Table 1 demonstrates the efficiency of the proposed model reduction method. One can see that for the decreasing tolerance, the dimension of the reduced-order system increases while the error in the output decreases. The speedup is defined as the simulation time for the original system divided by the simulation time for the reduced-order model. For example, a speedup of 219 in simulation of the reduced-order model of dimension $\hat{n} = 13$ with the error $\|\hat{y} - y\|_{\mathbb{L}_2(\mathbb{I})} = 6.2 \cdot 10^{-7}$ was achieved compared to the simulation of the original system. \triangleleft

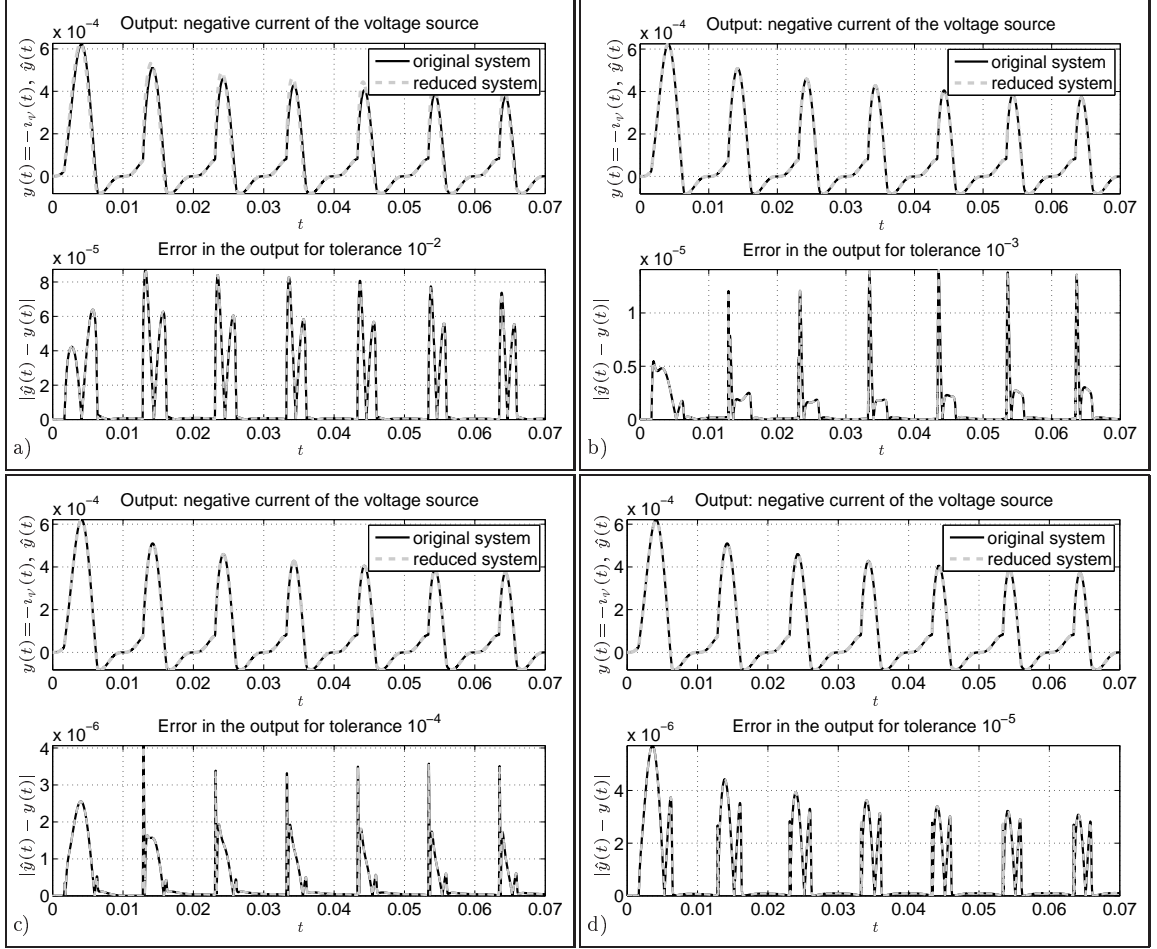


Figure 7: Outputs of the original and the reduced-order nonlinear systems and the errors in the output for the different tolerances a) 10^{-2} , b) 10^{-3} , c) 10^{-4} , d) 10^{-5} .

dimension of the original nonlinear system, n	1503	1503	1503	1503
simulation time for the original system, t_{sim}	24012s	24012s	24012s	24012s
tolerance for model reduction of the linear sub-system, tol	1e-02	1e-03	1e-04	1e-05
time for model reduction, t_{mor}	15s	24s	42s	61s
dimension of the reduced nonlinear system, \hat{n}	10	13	16	19
simulation time for the reduced system, \hat{t}_{sim}	82s	110s	122s	155s
error in the output, $\ \hat{y} - y\ _{\mathbb{L}_2(\mathbb{I})}$	7.0e-06	6.2e-07	2.0e-07	4.2e-07
speedup, $t_{\text{sim}}/\hat{t}_{\text{sim}}$	294.0	219.0	197.4	155.0

Table 1: Statistics for the RC circuit

Example 4.2 We consider now the nonlinear circuit shown in Figure 8. It contains 1000 repetitions of subcircuits consisting of 1 inductor, 2 capacitors and 2 resistors. Furthermore, at the beginning and at the end of the chain, we have a voltage source with $u_{\nu}(t) = \sin(100\pi t)^{10}\text{V}$ as in Figure 9 and an additional linear inductor, respectively. In the 1st, 101st, 201st, etc., subcircuits, a linear resistor is replaced by a diode, and in the 100th, 200th, 300th, etc., subcircuits, a linear inductor is replaced by a nonlinear inductor. The resulting nonlinear circuit contains 1 voltage source, 1990 linear resistors with $R_1 = 20\Omega$ and $R_2 = 1\Omega$, 991 linear inductors with $L = 0.01\text{H}$, 2000 linear capacitors with $C = 1\mu\text{F}$, 10 diodes with $\tilde{g}(u_{\tilde{x}}) = 10^{-14}(\exp(40\frac{1}{\sqrt{v}}u_{\tilde{x}}) - 1)\text{A}$, and 10 nonlinear inductors with

$$\tilde{\mathcal{L}}(i_{\tilde{L}}) = L_{\min} + (L_{\max} - L_{\min}) \exp(-i_{\tilde{L}}^2 L_{\text{scl}}),$$

where $L_{\min} = 0.001\text{H}$, $L_{\max} = 0.002\text{H}$ and $L_{\text{scl}} = 10^4\frac{1}{\text{A}}$. The state space dimension of the resulting DAE system is $n = 4003$.

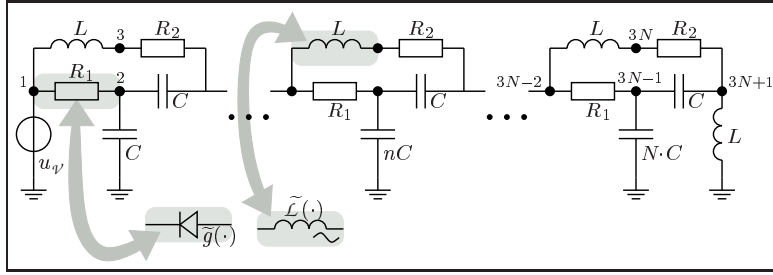


Figure 8: Nonlinear RLC circuit

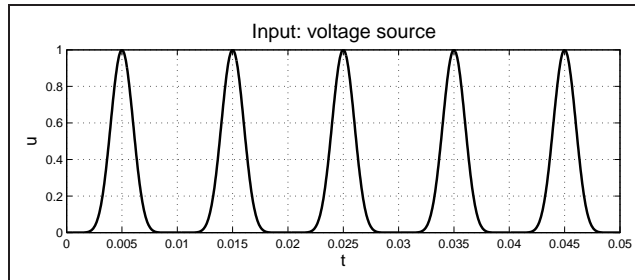


Figure 9: Voltage source for RLC circuit

The numerical simulation is done on the time interval $\mathbb{I} = [0\text{s}, 0.05\text{s}]$ using the BDF method of order 2 with a fixed stepsize of length $5 \cdot 10^{-5}\text{s}$. In Figure 10, we again present the outputs $y(t) = -i_{\nu}(t)$ and $\hat{y}(t)$ of the original and reduced-order nonlinear systems, respectively, as well as the error $|\hat{y}(t) - y(t)|$ for the different tolerances $tol = 10^{-2}, 10^{-3}, 10^{-4}, 10^{-5}$ for model reduction of the decoupled linear subcircuit. Table 2 demonstrates the efficiency of the model reduction method. As in the example above, also here one can see that if the

tolerance decreases, the dimension of the reduced-order system increases while the error in the output becomes smaller. In particular, for the approximate model of dimension $\hat{n} = 189$ with the error $\|\hat{y} - y\|_{\mathbb{L}_2(\mathbb{I})} = 4.10 \cdot 10^{-5}$, the simulation time is only 57 seconds instead of 1 hour and 13 minutes for the original system that implies a speedup of 76.8.

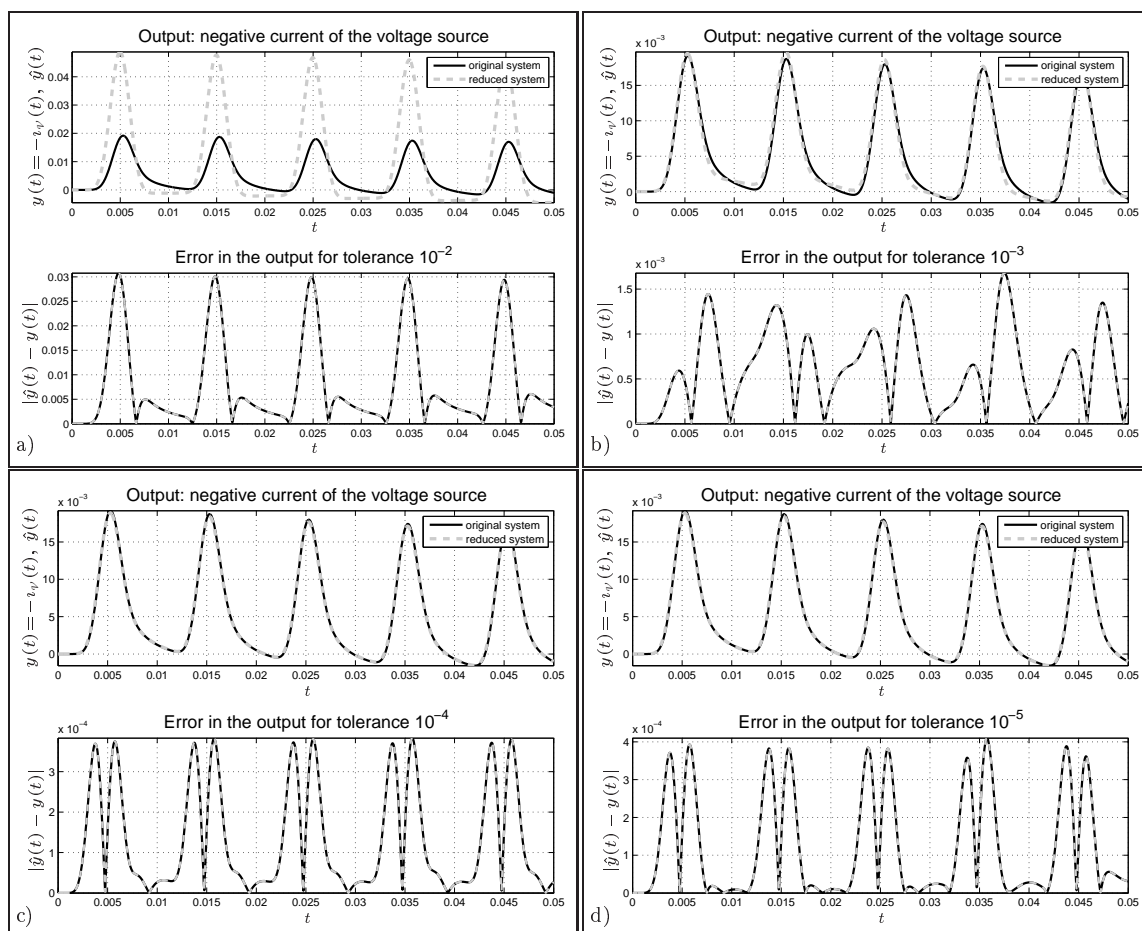


Figure 10: The outputs of the original and the reduced-order nonlinear systems and the errors in the output for the different tolerances a) 10^{-2} , b) 10^{-3} , c) 10^{-4} , d) 10^{-5} .

◀

5 Conclusion

In this paper, we developed a model order reduction method for large-scale nonlinear DAE systems arising in circuit simulation. This method is based on decoupling the electronic circuit into linear and nonlinear subcircuits followed by model reduction of the linear

dimension of the original nonlinear system, n	4003	4003	4003	4003
simulation time for the original system t_{sim}	4390s	4390s	4390s	4390s
tolerance for model reduction of the linear subsystem, tol	1e-02	1e-03	1e-04	1e-05
time for the model reduction, t_{mor}	2574s	2598s	2655s	2668s
dimension of the reduced nonlinear system, \hat{n}	127	152	189	218
simulation time for the reduced system, \hat{t}_{sim}	33s	42s	57s	74s
error in the output, $\ \hat{y} - y\ _{\mathbb{L}_2(\mathbb{I})}$	2.73e-03	1.67e-04	4.10e-05	4.09e-05
speedup, $t_{\text{sim}}/\hat{t}_{\text{sim}}$	132.0	104.1	76.8	59.1

Table 2: Statistics for the RLC circuit

part using a passivity-preserving balancing-related technique. Afterwards, the reduced-order linear model is recoupled with the unchanged nonlinear subsystem to obtain the reduced-order nonlinear model. We also analyzed the decoupling effects on the properties of the extracted linear subsystem. The efficiency and applicability of the considered model reduction approach was demonstrated on two numerical examples.

References

- [1] P. Benner and A. Schneider. Model order and terminal reduction approaches via matrix decomposition and low rank approximation. In J. Roos and L.R.J. Costa, editors, *Scientific Computing in Electrical Engineering SCEE 2008*, volume 14 of *Mathematics in Industry*, pages 523–530. Springer-Verlag, Berlin, Heidelberg, 2010.
- [2] K.E. Brenan, S.L. Campbell, and L.R. Petzold. *The Numerical Solution of Initial-Value Problems in Differential-Algebraic Equations*. Classics in Applied Mathematics, 14. SIAM, Philadelphia, PA, 1996.
- [3] D. Estévez Schwarz and C. Tischendorf. Structural analysis for electric circuits and consequences for MNA. *Int. J. Circ. Theor. Appl.*, 28:131–162, 2000.
- [4] P. Feldmann and F. Liu. Sparse and efficient reduced order modeling of linear subcircuits with large number of terminals. In *Proceedings of the 2004 IEEE/ACM International Conference on Computer-Aided Design (ICCAD'04)*, pages 88–92, Washington, DC, 2004.
- [5] R.W. Freund. Reduced-order modeling techniques based on Krylov subspaces and their use in circuit simulation. In B.N. Datta, editor, *Applied and Computational Control, Signals, and Circuits*, volume 1, pages 435–498. Birkhäuser, Boston, 1999.

- [6] R.W. Freund. SPRIM: structure-preserving reduced-order interconnect macromodeling. In *Proceedings of the 2004 IEEE/ACM International Conference on Computer-Aided Design (ICCAD'04)*, pages 80–87, Los Alamos, CA, 2004.
- [7] R.W. Freund. Structure-preserving model order reduction of RCL circuit equations. In W.H.A. Schilders, H.A. van der Vorst, and J. Rommes, editors, *Model Order Reduction: Theory, Research Aspects and Applications*, volume 13 of *Mathematics in Industry*, pages 49–73. Springer-Verlag, Berlin, Heidelberg, 2008.
- [8] E. Griepentrog and R. März. *Differential-Algebraic Equations and Their Numerical Treatment*. Teubner-Texte zur Mathematik, 88. B.G. Teubner, Leipzig, 1986.
- [9] M. Heinkenschloss and T. Reis. Model reduction for a class of nonlinear electrical circuits by reduction of linear subcircuits. Technical Report 702-2010, DFG Research Center MATHEON, Technische Universität Berlin, 2010.
- [10] R. Ionutiu and J. Rommes. On synthesis of reduced order models. In P. Benner, M. Hinze, and E.J.W ter Maten, editors, *Model Reduction for Circuit Simulation*, volume 74 of *Lecture Notes in Electrical Engineering*, pages 201–214. Springer-Verlag, Berlin, Heidelberg, 2011.
- [11] P. Kunkel and V. Mehrmann. *Differential-Algebraic Equations. Analysis and Numerical Solution*. EMS Publishing House, Zürich, Switzerland, 2006.
- [12] P. Liu, S.X.D. Tan, B. Yan, and B. McGaughy. An efficient terminal and model order reduction algorithm. *Integr. VLSI J.*, 41(2):210218, 2008.
- [13] A. Odabasioglu, M. Celik, and L.T. Pileggi. PRIMA: Passive reduced-order interconnect macromodeling algorithm. *IEEE Trans. Circuits Syst.*, 17(8):645–654, 1998.
- [14] J. R. Phillips. Projection-based approaches for model reduction of weakly nonlinear, time-varying systems. *IEEE Trans. Computer-Aided Design Integr. Circuits Syst.*, 22(2):171–187, 2003.
- [15] T. Reis. Circuit synthesis of passive descriptor systems - a modified nodal approach. *Internat. J. Circuit Theory Appl.*, 38(1):44–68, 2010.
- [16] T. Reis and T. Stykel. Positive real and bounded real balancing for model reduction of descriptor systems. *Internat. J. Control*, 83(1):74–88, 2009.
- [17] T. Reis and T. Stykel. PABTEC: Passivity-preserving balanced truncation for electrical circuits. *IEEE Trans. Computer-Aided Design Integr. Circuits Syst.*, 29(9):1354–1367, 2010.
- [18] T. Reis and T. Stykel. Lyapunov balancing for passivity-preserving model reduction of RC circuits. *SIAM J. Appl. Dyn. Syst.*, 10(1):1–34, 2011.

- [19] M.J. Rewieński. *A Trajectory Piecewise-Linear Approach to Model Order Reduction of Nonlinear Dynamical Systems*. Ph.D. thesis, Massachusetts Institute of Technology, 2003.
- [20] M. Striebel and J. Rommes. Model order reduction of nonlinear systems in circuit simulation: status and applications. In P. Benner, M. Hinze, and E.J.W ter Maten, editors, *Model Reduction for Circuit Simulation*, volume 74 of *Lecture Notes in Electrical Engineering*, pages 279–292. Springer-Verlag, 2011.
- [21] T. Stykel. Balancing-related model reduction of circuit equations using topological structure. In P. Benner, M. Hinze, and E.J.W ter Maten, editors, *Model Reduction for Circuit Simulation*, volume 74 of *Lecture Notes in Electrical Engineering*, pages 53–80. Springer-Verlag, Berlin, Heidelberg, 2011.
- [22] P. Triverio, S. Grivet-Talocia, M.S. Nakhla, F. Canavero, and R. Achar. Stability, causality, and passivity in electrical interconnect models. *IEEE Trans. Adv. Packaging*, 30(4):795–808, 2007.
- [23] A. Verhoeven, J. ter Maten, M. Striebel, and R. Mattheij. Model order reduction for nonlinear IC models. In A. Korytowski, K. Malanowski, W. Mitkowski, and M. Szymkat, editors, *System Modeling and Optimization*, volume 312 of *IFIP Advances in Information and Communication Technology*, pages 476–491. Springer-Verlag, 2010.
- [24] J. Vlach and K. Singhal. *Computer Methods for Circuit Analysis and Design*. Van Nostrand Reinhold, New York, 1994.
- [25] F. Yang, X. Zeng, Y. Su, and D. Zhou. RLC equivalent circuit synthesis method for structure-preserved reduced-order model of interconnect in VLSI. *Commun. Comput. Phys.*, 3(2):376–396, 2008.